

## Research Article

# Ligustrazine Prevents Intervertebral Disc Degeneration via Suppression of Aberrant TGF $\beta$ Activation in Nucleus Pulposus Cells

Shufen Liu,<sup>1</sup> Yuhao Cheng,<sup>2</sup> Yuqi Tan,<sup>2</sup> Jingcheng Dong<sup>1,3</sup> ,<sup>3</sup> and Qin Bian<sup>1,3</sup> 

<sup>1</sup>Longhua Hospital, Shanghai University of Traditional Chinese Medicine, Shanghai, China

<sup>2</sup>Institute for Cell Engineering, Johns Hopkins University School of Medicine, Baltimore, MD, USA

<sup>3</sup>The Institutes of Integrative Medicine, Fudan University, Shanghai, China

Correspondence should be addressed to Jingcheng Dong; [jcdong2004@126.com](mailto:jcdong2004@126.com) and Qin Bian; [bianqin213@gmail.com](mailto:bianqin213@gmail.com)

Received 7 June 2019; Revised 10 August 2019; Accepted 23 August 2019; Published 2 December 2019

Academic Editor: William B. Rodgers

Copyright © 2019 Shufen Liu et al. This is an open access article distributed under the Creative Commons Attribution License, which permits unrestricted use, distribution, and reproduction in any medium, provided the original work is properly cited.

**Objectives.** Aberrant transforming growth factor  $\beta$  (TGF $\beta$ ) activation is detrimental to both nucleus pulposus (NP) cells and cartilage endplates (CEPs), which can lead to intervertebral disc degeneration (IDD). Ligustrazine (LIG) reduces the expression of inflammatory factors and TGF $\beta$ 1 in hypertrophic CEP to prevent IDD. In this study, we investigate the effects of LIG on NP cells and the TGF $\beta$  signaling. **Design.** LIG was injected to the lumbar spinal instability (LSI) mouse model. The effect of LIG was evaluated by intervertebral disc (IVD) score in the LSI mouse model. The expression of activated TGF $\beta$  was examined using immunostaining with pSmad2/3 antibody. The upright posture (UP) rat model was also treated and evaluated in the same manner to assess the effect of LIG. In *ex vivo* study, IVDs from four-week old mice were isolated and treated with  $10^{-5}$ ,  $10^{-6}$ , and  $10^{-7}$  M of LIG. We used western blot to detect activated TGF $\beta$  expression. TGF $\beta$ -treated human nucleus pulposus cells (HNPCs) were cotreated with optimized dose of LIG *in vitro*. Immunofluorescence staining was performed to determine pSmad2/3, connective tissue growth factor (CCN2), and aggrecan (ACAN) expression levels. **Results.** IVD score and the percentage of pSmad2/3+ NP cells were low in LIG-treated LSI mice in comparison with LSI mice, but close to the levels in the Sham group. Similarly, LIG reduced the overexpression of TGF $\beta$ 1 in NP cells. The inhibitory effect of LIG was dose dependent. A dose of  $10^{-5}$  M LIG not only strongly attenuated Smad2/3 phosphorylation in TGF $\beta$ -treated IVD *ex vivo* but also suppressed pSmad2/3, CCN2, and ACAN expression in TGF $\beta$ -treated NP cells *in vitro*. **Conclusions.** LIG prevents IDD via suppression of TGF $\beta$  overactivation in NP cells.

## 1. Introduction

Nucleus pulposus (NP) cells reside in the center of intervertebral disc (IVD) and play a key role in development of intervertebral disc degeneration (IDD) [1]. Mechanical loading triggers IDD by accelerating NP shrinkage and subsequently transits to fibroblast-like cells, which have decreased capacities in maintenance of IVD plasticity [2].

Ligustrazine (LIG) is an extract from *Ligusticum wallichii* Franchat (Chuanxiong), which is a traditional Chinese herb known for its wide usage in treating spinal degenerative diseases [3]. Two clinical trials (680 participants) found a compound that contains Chuanxiong, which relieved neck pain better in the short term than placebo in cervical IDD

patients. One trial (60 participants) indicated an oral herbal formula with the component of Chuanxiong, which relieved pain better than Mobicox or Methycobal in treatment for cervical IDD [4]. An animal experiment revealed herb formula “Fufangqishe-Pill,” which prevents upright posture- (UP-) induced lumbar IDD in the rat model [5]. Further study showed the main effective component of “Fufangqishe-Pill,” LIG, decelerates the progression of lumbar IDD through inhibiting inflammatory factors such as IL-1 $\beta$ , COX-2, and iNOS in the upright posture (UP) rat model [6]. In addition to anti-inflammation effect, a standard traditional Chinese medicine library screening showed LIG exerts an antifibrosis effect via inhibition of TGF $\beta$  [7]. Since IDD is also considered as a transition of fibrosis, we hypothesize

that prevention of IDD by LIG is related to regulation of TGF $\beta$  signaling.

Our previous work found the overexpression of TGF $\beta$  accelerates cartilage endplate (CEP) hypertrophy and NP cell dysfunction, leading to IDD [2, 8]. Interestingly, LIG prevents CEP outgrowth and suppresses TGF $\beta$ 1 expression in hypertrophic CEP of IDD rats [9]. However, whether LIG has an antifibrotic effect on NP cells is not known. To investigate the effects of LIG on NP cells and explore its potential mechanism involving in TGF $\beta$  signaling, we employed two IDD animal models to investigate the effects of LIG on NP cells and TGF $\beta$  levels in different species and different mechanical loading patterns. We then isolated IVD from 4-week old mice and tested the dose response of LIG on TGF $\beta$  signaling by western blot *ex vivo*. The optimized dose of LIG was further applied to NP cells *in vitro* to determine the TGF $\beta$  signal downstream target gene expression of CCN2 and ACAN.

## 2. Materials and Methods

**2.1. LIG Preparation.** Ligustrazine phosphate (purity > 99%, MW: 252.21) was purchased from the Chinese Medicine and Biological Products Institute (Beijing, China). The solutions of ligustrazine phosphate were prepared in dimethylsulfoxide (DMSO, Sigma, USA) and diluted with culture media for the *in vitro* experiments. The final concentration of DMSO was no more than 0.1%.

**2.2. Animal Models and LIG Administration.** After intraperitoneal injection, anesthetized with ketamine (80 mg/kg) and xylazine (5 mg/kg), the 3rd–5th lumbar (L3–L5) spinous processes along with the supraspinous and interspinous ligaments of the 8-week old male C57BL/6J mice (28 g  $\pm$  5 g, Shanghai Laboratory Animal Center, China) were resected to induce the lumbar spine instability (LSI) mouse model. Sham operations were carried out only by detaching the posterior paravertebral muscles from the L3–L5 vertebrae. The operated mice were then intraperitoneally injected with ligustrazine hydrochloride (Nanning Maple Leaf Pharmaceutical Co., Ltd, China, 1 mL, 2 mg/d/per mouse) while the mice operated in the sham surgery were injected with the equal volume of saline solution at the same frequency and duration (once a day for one month). Protocol #PZSHUTCM190315024 was approved by the Shanghai University of Traditional Chinese Medicine Animal Care and Use Committee.

Sprague-Dawley (SD) (male, 1-month old, 200 g  $\pm$  20 g) rats (Shanghai Laboratory Animal Center, China) were anesthetized with 100 mg/kg ketamine by intraperitoneal injection. The forelimb surgery and customized cages force them to stand up which triggers IDD initiation as previously described [10]. Ligustrazine hydrochloride was administered as described above (16 mL/kg-d, 4 mg/mL). Their lumbar spines were later dissected for further analysis. Protocol #PZSHUTCM190315024 was approved by the Shanghai University of Traditional Chinese Medicine Animal Care and Use Committee.

All animals were randomly divided into each group. All surgeries were performed in the laboratory, and drug administration was done in the animal facility. Animals were sacrificed before sample collection with CO<sub>2</sub> exposure followed by cervical dislocation.

**2.3. IVD Ex Vivo Model.** The L1–L5 lumbar IVDs were removed under sterile conditions from 4-week-old C57BL/6J male mice (20 g  $\pm$  2 g, Shanghai Laboratory Animal Center, China). The collected IVDs were cultured in Dulbecco's Modified Eagle Medium (DMEM, Invitrogen, Carlsbad, CA, USA) supplemented with 1% penicillin-streptomycin (MediaTech, Dallas, TX, USA). The culture was then treated with 2 ng/mL of recombinant mouse TGF $\beta$ 1 with added LIG mixture at 0, 10<sup>-7</sup> M, 10<sup>-6</sup> M or 10<sup>-5</sup> M dosage, respectively, overnight (rmTGF $\beta$ 1, 7666-MB-005, R&D, Minneapolis, MN, USA).

**2.4. In Vitro Experiment.** Human nucleus pulposus cells (HNPCs) were purchased from ScienCell research Laboratories (Catalog #4800) and were cultured with DMEM, 10% fetal bovine serum (FBS), and 1% penicillin-streptomycin. When the HNPC culture reached 70% confluency, they were starved by replacing 10% FBS DMEM culture medium with FBS-free culture medium for 24 h. Then, the HNPC cells were treated with 5 ng/mL rmTGF $\beta$ 1 combined with or without 10<sup>-5</sup> M LIG or 0.01% DMSO (rmTGF $\beta$ 1 + Veh) for another 48 h.

**2.5. Histochemistry, Immunohistochemistry, and Histomorphometry.** The mice and rat specimens were fixed in 10% buffered formalin for 48 h, decalcified in 10% ethylenediaminetetraacetic acid (EDTA) (pH 7.4) for 14 days and 20% EDTA for 4 weeks, respectively, dehydrated, and embedded in paraffin. The mice specimens and the rat specimens of the L4-L5 spines were sectioned at 4  $\mu$ m and 7  $\mu$ m, respectively, and stained with Safranin O and fast green. Sections were incubated with primary antibodies to pSmad2/3 (1 : 200, sc-11769, Santa Cruz Biotechnology, Inc., Dallas, TX, USA), TGF $\beta$ 1 (1 : 100, Cell Signaling Technology Inc., MA, USA), ACAN (1 : 200, AB1031, MilliporeSigma, Billerica, MA, USA), CCN2 (1 : 400, ab6992, Abcam) at 4°C overnight. For immunohistochemical staining, a horseradish peroxidase-streptavidin detection system (Dako, Carpinteria, CA, USA) was subsequently used to detect the immunoactivity, followed by counterstaining with hematoxylin (Sigma-Aldrich). For the immunofluorescent assay, the slides were incubated with conjugated secondary antibodies conjugated at room temperature for 1 h while avoiding light and counterstained with 2-(4aminodiphenyl)-6-indolecarbamide dihydrochloride (DAPI). Morphometric study was performed by an image autoanalysis system (Olympus DP71).

**2.6. Quantitative Histomorphometric Analysis.** Quantitative histomorphometric analysis was conducted with Image-Pro Plus software version 6.0 (Media Cybernetics Inc., Rockville, MD, USA). IVD scores were obtained as described

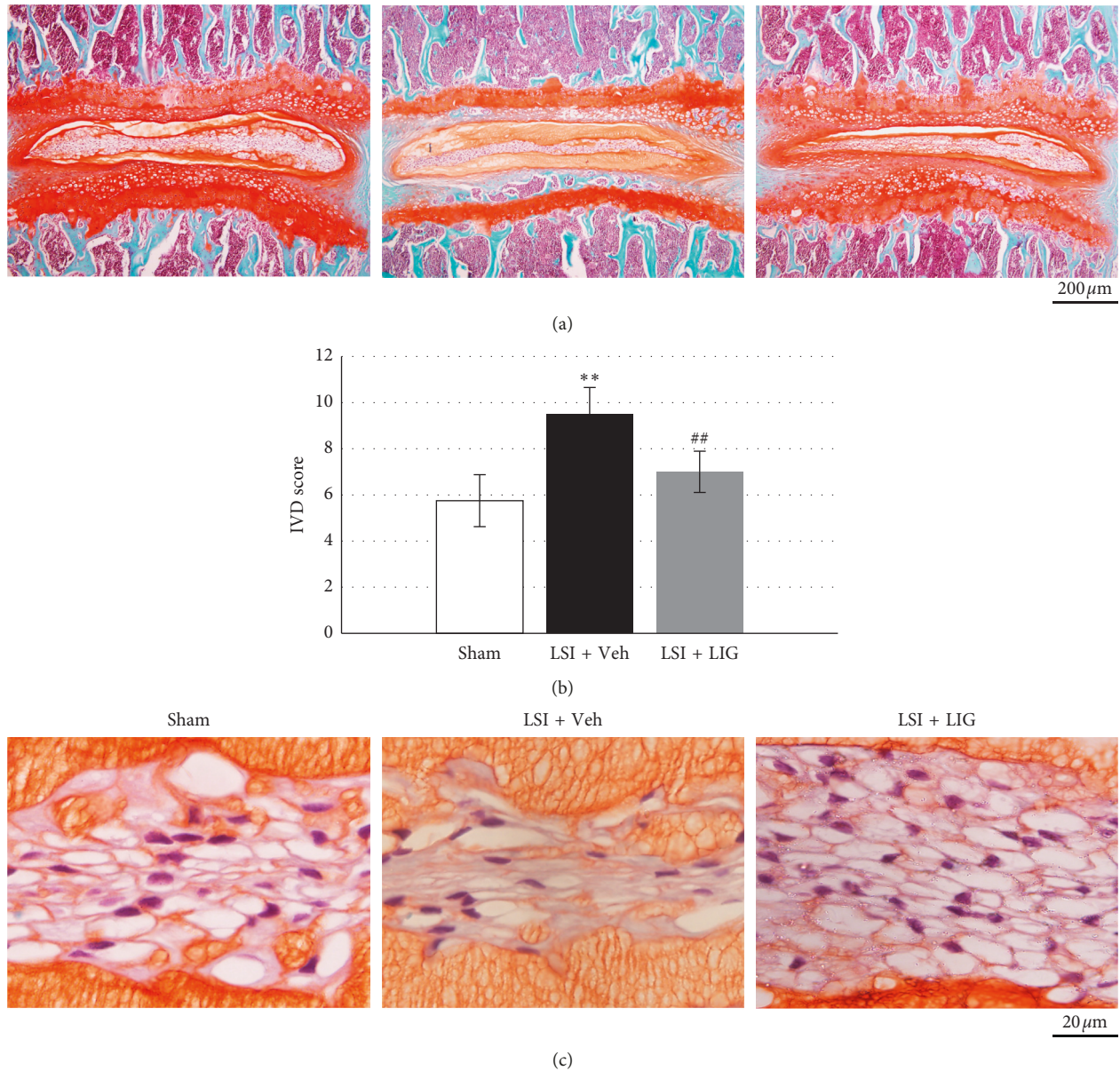


FIGURE 1: The effect of LIG on NP cell vacuoles and IVD score in LSI mice. (a) Representative images of the whole IVD sections in the LSI-induced mice model stained with Safranin O and fast green. (b) IVD score evaluated 4 weeks after LSI surgery. (c) Representative Safranin O staining images of the IVD sections showing the changes of NC cells in LSI + Veh, LSI + LIG, and sham-operated 8-week-old mice at 4 weeks after surgery. Each column represents the mean ± SE.  $n = 10$  per group. \*\*  $p < 0.01$  vs Sham, ##  $p < 0.01$  vs LSI + Veh.

previously [11]. In detail, the organization of annulus fibrosus (AF), border between the AF and NP, cellularity of the NP, and matrix of the NP were assessed. The percentage of pSmad2/3-positive cells was obtained by counting the number of positive staining cells and the total number of cells in the NP region. The area of TGFβ1-positive staining was calculated by measuring the positive staining area of region of interest that covers all cells in NP. The area of CCN2+ or ACAN+ per cell was measured by dividing the total positive staining area of CCN2 or ACAN+ by total cell numbers. Dividing the total positive staining area by total cell nucleus area, we get the percentage of pSmad2/3+ area per cell.

**2.7. Western Blot.** The cellular extraction from NP tissue in *ex vivo* assay was analyzed with a western blot. The cellular extraction was centrifuged, and the concentration of supernatants was evaluated by the DC protein assay (Bio-Rad Laboratories, Hercules, CA, USA), and then the proteins were separated by SDS-polyacrylamide gel electrophoresis and blotted on a polyvinylidene fluoride membrane (Bio-Rad Laboratories). After incubation in antibodies, proteins were detected using an enhanced chemiluminescence kit (Amersham Biosciences, Pittsburgh, PA, USA). The target protein expression was examined with the following antibodies: mouse pSmad2 (1:1000, 3101, Cell Signaling Technology Inc., Danvers, MA, USA), Smad2 (1:1000, 3103,

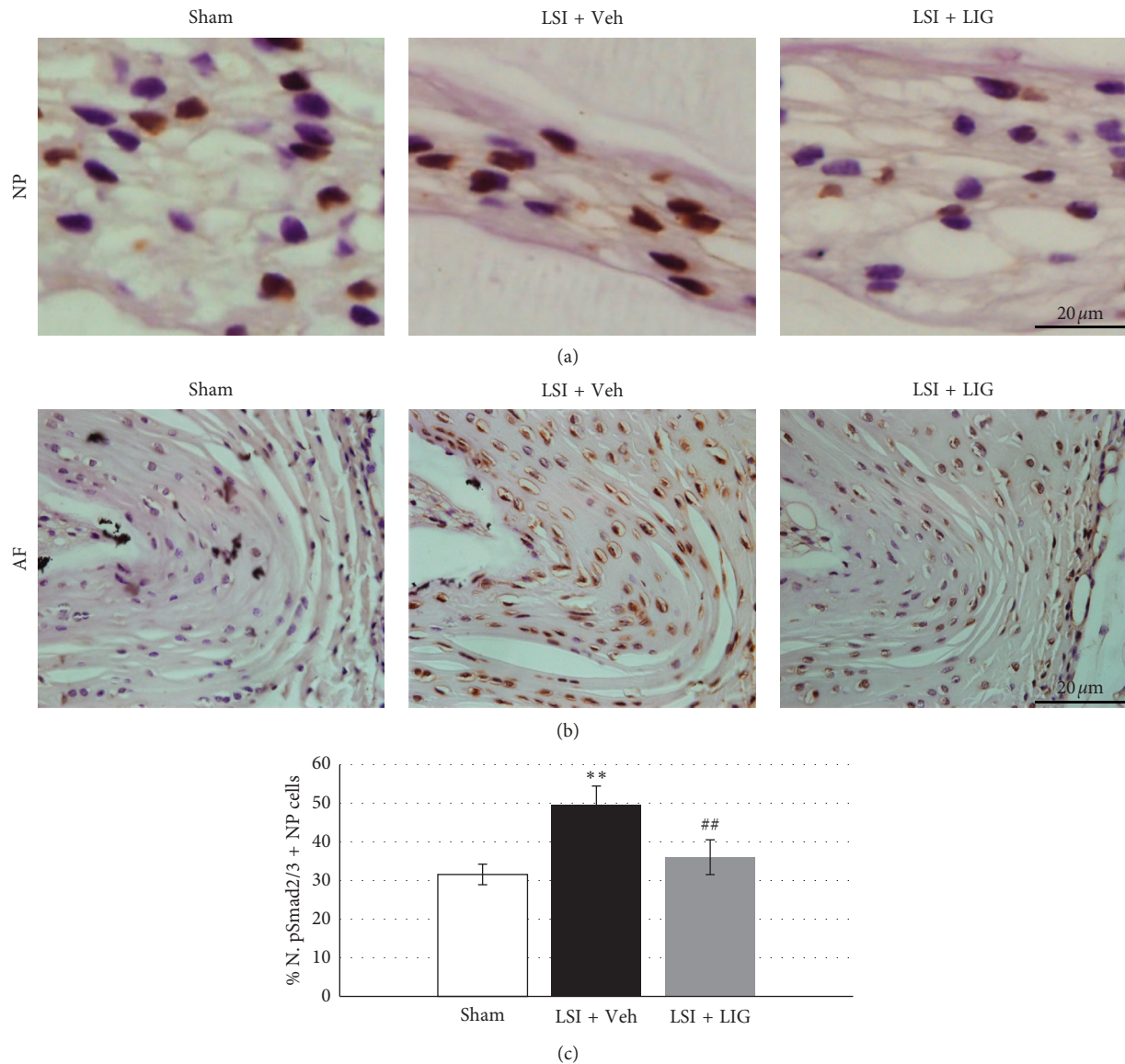


FIGURE 2: The effect of LIG on TGF $\beta$  activation in NP cells of LSI mice. (a) Representative immunostaining images of IVD sections with antibody against pSmad2/3 (brown). Hematoxylin stains the nuclei purple. (b) Quantification of pSmad2/3+ cells in (c). Each column represents the mean  $\pm$  SE.  $n = 8$  per group. \*\* $p < 0.01$  vs Sham, ## $p < 0.01$  vs LSI + Veh.

Cell Signaling Technology Inc.), and GAPDH (1:1 000, 8884, Cell Signaling Technology Inc.).

**2.8. Statistical Analyses.** The data are expressed as means  $\pm$  standard error (SE), and statistical significance was calculated using one-way analysis of variance (ANOVA) followed by a post hoc LSD test (homogeneity of variance) and Tukey's test (heterogeneity of variance) using SPSS software (SPSS Inc., Chicago, USA). The significance level was defined as  $p < 0.05$ .

### 3. Results

**3.1. LIG Maintains NP Cell Vacuoles and IVD Score in LSI Mice.** The effect of LIG on NP cells *in vivo* was assessed by

using the LSI mice model. LSI surgery induced significant IDD as shown by IVD score after 4 weeks. LIG treatment increased IVD score compared with vehicle (Veh) treatment (Figures 1(a) and 1(b)). Safranin O staining showed reduced vacuole sizes in NP cells after LSI surgery, whereas in the case where LSI mice were treated with LIG, the vacuole sizes were similar to those in Sham mice (Figure 1(c)). The maintenance of IVD score and NP cells' vacuole sizes indicated LIG preventing IDD progression.

**3.2. LIG Decreases TGF $\beta$  Activation in NP Cells of LSI Mice.** Vacuole sizes of NP cells are regulated by TGF $\beta$  activation. To investigate the effect of LIG on TGF $\beta$  activation during LSI-induced IDD, we examine the activation of TGF $\beta$  with the immunochemical assay. It showed latent TGF $\beta$  was

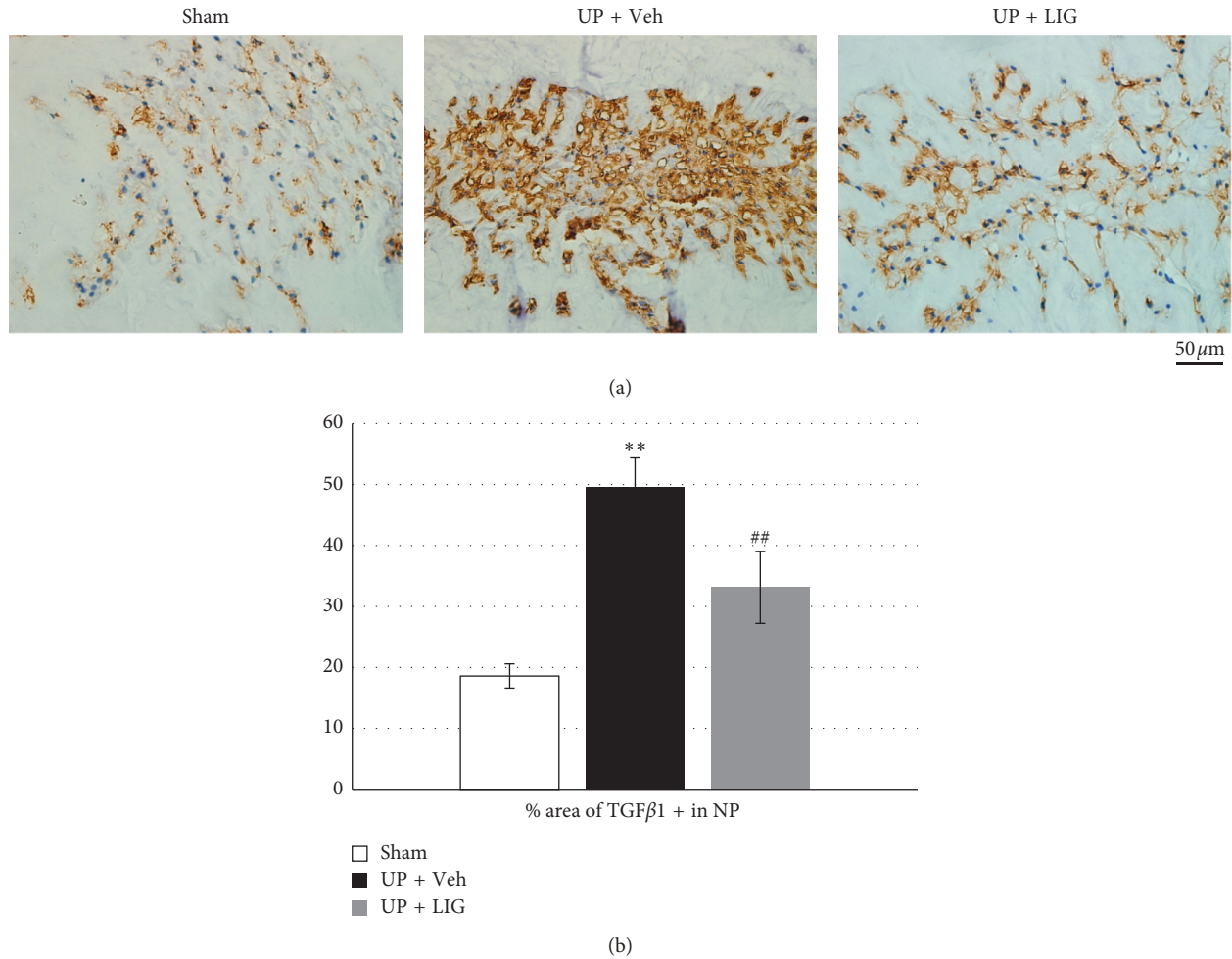


FIGURE 3: The effect of LIG on TGFβ1 expression in NP of UP rats. (a) Representative immunostaining images of IVD sections with antibody against TGFβ1 (brown). Hematoxylin stains the nuclei purple. (b) Quantification of TGFβ1+ area vs NP area in (a). Each column represents the mean ± SE. n = 8 per group. \*\* p < 0.01 vs Sham, ## p < 0.01 vs UP + Veh.

activated after LSI surgery, indicated by significantly increased phosphorylated Smad2/3-positive (pSmad2/3+) cells in NP and annulus fibrosus (AF) (Figures 2(a)–2(c)). Decreased pSmad2/3+ cells were observed in the LIG treatment group relative to those in the Veh treatment group (Figures 2(a)–2(c)).

**3.3. LIG Reduces TGFβ1 Expression in NP Cells of UP Rats.** To test the effect of LIG on NP cells in different animal models, we employed a rat model in which IDD is induced by upright posture [10]. We found that TGFβ expressions were significantly increased in NP cells of the UP + Veh group relative to the Sham group (Figures 3(a) and 3(b)). Continuous LIG treatment for 1 month significantly decreased TGFβ expressions in NP cells relative to Veh treatment (Figures 3(a) and 3(b)).

**3.4. The Effects of LIG on TGFβ Activation in IVD Are Dose-Dependent.** To test whether the effects of LIG on TGFβ

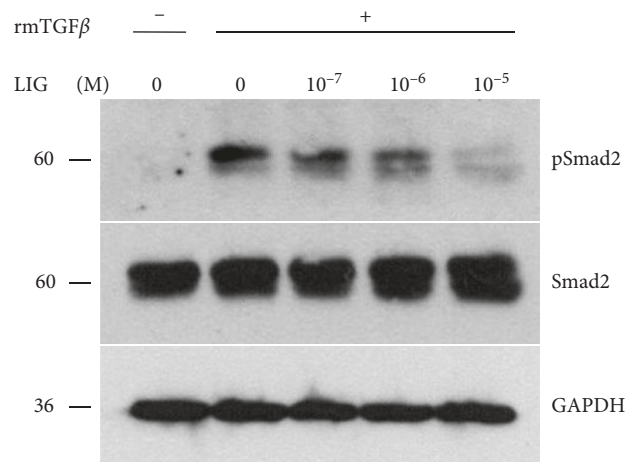
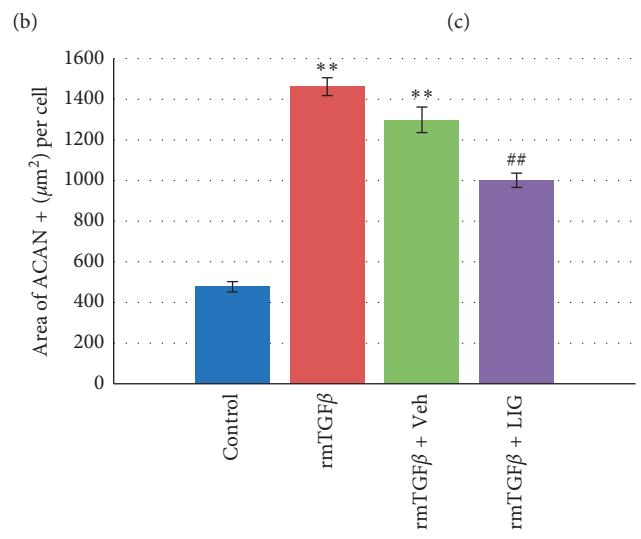
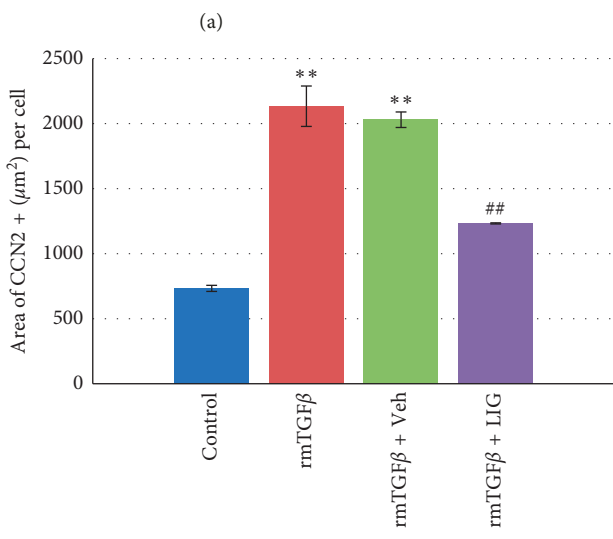
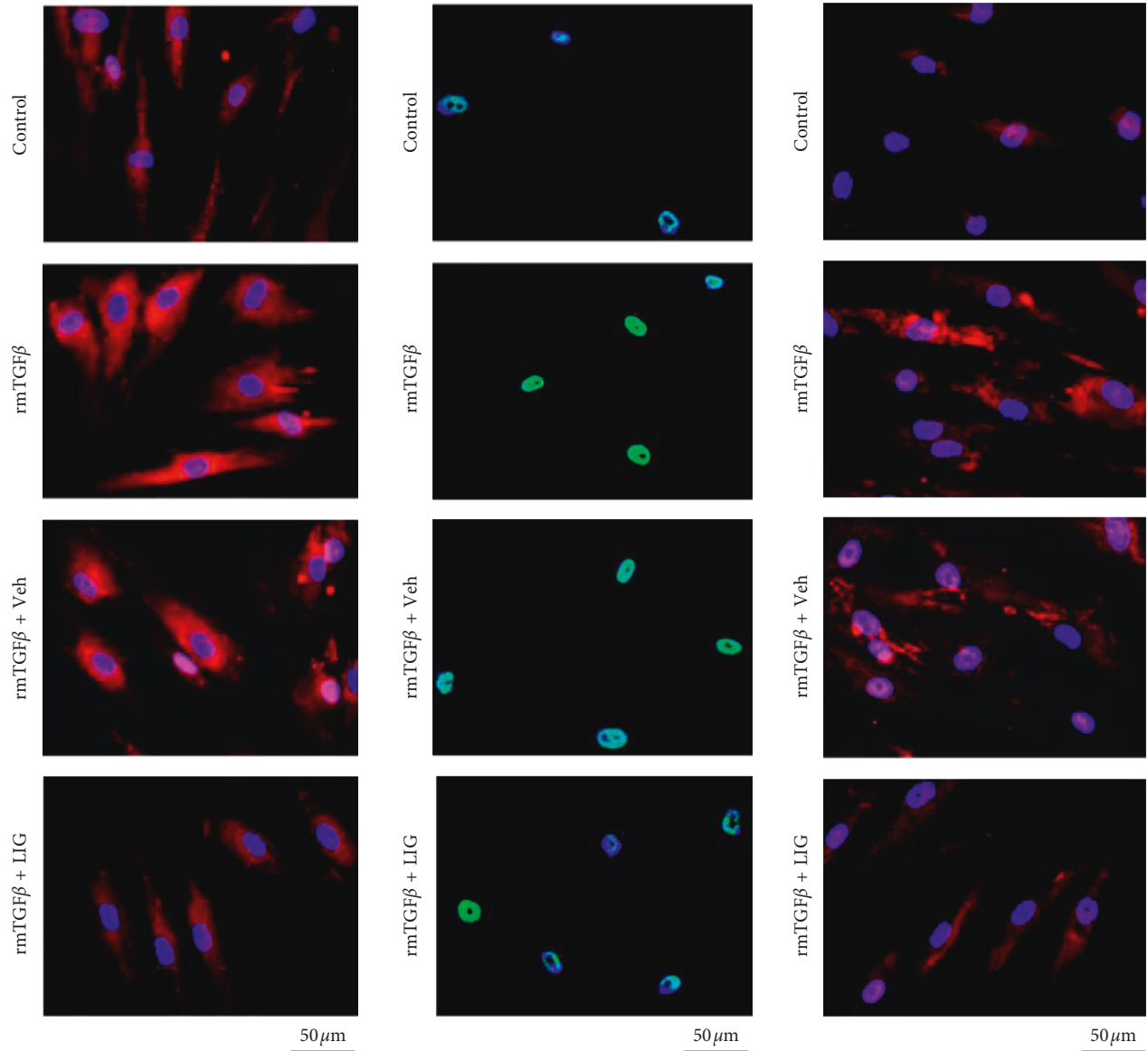


FIGURE 4: The dose-dependent effect of LIG on TGFβ activation in mouse IVD ex vivo. Western blot analysis of pSmad2 and total Smad2 levels in the IVD, pretreated with 2 ng/mL of rmTGFβ1 combined with 10<sup>-5</sup>, 10<sup>-6</sup>, and 10<sup>-7</sup> M LIG.



(d)

(e)

FIGURE 5: Continued.

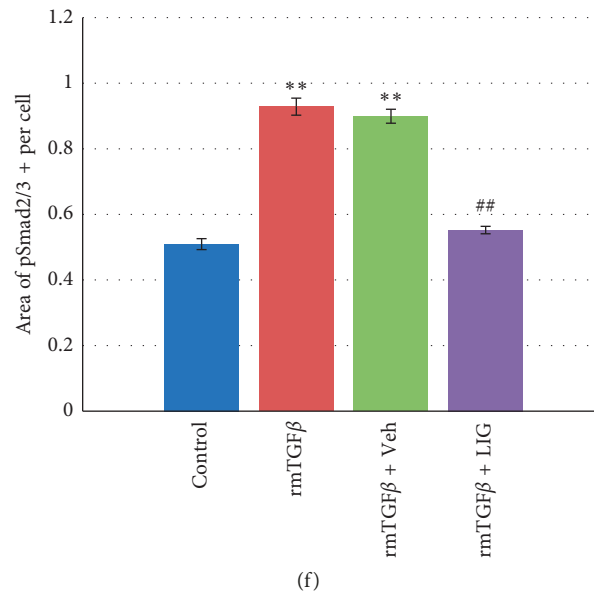


FIGURE 5: The effect of LIG on HNPC *in vitro*. (a–c) Representative immunostaining images of HNPC treated with 5 ng/mL rmTGFβ1 combined with or without 10<sup>-5</sup> M LIG, or 0.01% DMSO (rmTGFβ1 + Veh) for CCN2 (a), pSmad2/3 (b), and ACAN (c). (d–f) Quantification of CCN2, pSmad2/3, and ACAN expressions in (a)–(c). Each column represents the mean ± SE of three independent experiments. \*\**p* < 0.01 vs Control, ##*p* < 0.01 vs rmTGFβ.

activation are dose-dependent, we applied different doses of LIG on TGFβ pretreated IVD *ex vivo*. After 24 h, the protein levels of pSmad2 were significantly increased by TGFβ induction. The combination of LIG treatment decreased the levels of pSmad2 in a dose-dependent pattern. The dose of 10<sup>-5</sup> M LIG exerted the most significant inhibitory effect on pSmad2 levels that were stimulated by exogenous TGFβ (Figure 4). This dose is chosen for further *in vitro* experiment.

**3.5. LIG Inhibits TGFβ Downstream Factors CCN2 and ACAN in NP Cells.** We then investigate the effect of LIG on TGFβ downstream factors *in vitro*. The levels of CCN2, which upregulates the synthesis of matrix proteins in IVDs [12–15], were significantly increased by exogenous TGFβ induction (Figures 5(a) and 5(d)). The result is consistent with the increase of TGFβ activity indicated by increased pSmad2/3+ cells (Figures 5(b) and 5(e)). Similarly, ACAN expression, upregulated by CCN2 [12, 16], was also increased in TGFβ-stimulated NP cells (Figures 5(c) and 5(f)). As expected, the combination of 10<sup>-5</sup> M of LIG treatment decreased the expressions of CCN2, ACAN, and pSmad2/3 in NP cells, indicating LIG inhibited TGFβ activity (Figures 5(a)–5(f)).

## 4. Discussion

Nucleus pulposus cells, a remnant of embryonic notochord, are a unique cell type present in compartment of IVDs [17]. Overactivation of TGFβ is a key molecular event that mediates NP cell transition, leading to IDD development. Recently, new therapies have been reported to prevent IDD via targeting NP

cells and extracellular matrix remodeling such as microRNA-based therapy and melatonin [18, 19]. However, the therapy targeting NP cells through TGFβ activity has not been reported.

Our study revealed that LIG prevented NP cell transition and maintained vacuole sizes of NP cells. LIG was reported to exert chondroprotective effect by inhibiting chondrocytes apoptosis [20], attenuating the interleukin 1β (IL-1β)-induced Glycosaminoglycan (GAG) degradation and matrix metalloproteinase-3 (MMP-3) expression, increasing cell viability through suppression of ROS production, maintaining mitochondrial membrane potential, and downregulating caspase-3 activity [21]. It is also a potent blocker of vasoconstriction and a strong scavenger of oxygen-free radicals. LIG enhances vascularization by increasing vessel volume, vessel surface, and vessel thickness, upregulating vascular endothelial growth factor (VEGF) in femoral heads [22]. However, LIG is barely able to increase vascularization on NP cells since NP cells are avascular.

We found the effect of LIG on NP cells is associated with inhibition of TGFβ overactivation and TGFβ1 expression, which is similar to several reports on other organs or cell types. For example, LIG decreases the expression of TGFβ1 and reduces deposition of type III collagen during airway remodeling [23]. It also resists renal interstitial fibrosis by downregulation of TGFβ1 and CCN2 and upregulation of Smad7 [24, 25]. LIG prevents and alleviates the development of liver fibrosis by downregulating TGFβ1, TβRII, CCN2, and Smad2/3, and type I collagen while upregulating Smad7 [26, 27] and inhibits proliferation of hepatic stellate cells [28]. LIG prevents post-operative intra-abdominal adhesions by inhibition of pSmad2/3

expression and increasing the level of Smad7 in the peritoneal mesothelial cells [29]. Collectively, LIG prevents IDD via modulating TGF $\beta$  signal.

There are also some limitations in our study. We observed the effect of LIG on animal models for one month which is relatively short. Long-term effect has not been assessed in this study. The potential downsides of long-term treatment may include antifibrotic effect on tissue repair such as scar tissue formation.

## 5. Conclusion

LIG prevents NP cell transition by suppression of TGF $\beta$  overactivation. It can be developed as a therapeutic alternative for IDD.

## Data Availability

The data used to support the findings of this study are included within the article.

## Conflicts of Interest

The authors declare that they have no conflicts of interest.

## Authors' Contributions

SFL and QB conducted experiments. YHC and YQT edited the manuscript. JCD and QB designed the project. QB prepared the manuscript.

## Acknowledgments

This study was supported by the Project of National Natural Science Foundation of China (Award #81573992) and the Development Project of Shanghai Peak Disciplines-Integrative Medicine (Award #20150407).

## References

- [1] D. Sakai, Y. Nakamura, T. Nakai et al., "Exhaustion of nucleus pulposus progenitor cells with ageing and degeneration of the intervertebral disc," *Nature Communications*, vol. 3, no. 1, p. 1264, 2012.
- [2] Q. Bian, L. Ma, A. Jain et al., "Mechanotransduction activation of TGF $\beta$  maintains intervertebral disc homeostasis," *Bone Research*, vol. 5, no. 1, p. 17008, 2017.
- [3] S. Imagama, Y. Hasegawa, T. Seki et al., "The effect of beta-carotene on lumbar osteophyte formation," *Spine*, vol. 36, no. 26, pp. 2293–2298, 2011.
- [4] X. Cui, K. Trinh, and Y. J. Wang, "Chinese herbal medicine for chronic neck pain due to cervical degenerative disc disease," *Cochrane Database of Systematic Reviews*, vol. 20, no. 1, Article ID CD006556, 2010.
- [5] Q.-Q. Liang, Z.-J. Xi, Q. Bian et al., "Herb formula 'Fufangqishe-Pill' prevents upright posture-induced intervertebral disc degeneration at the lumbar in rats," *Journal of Pharmacological Sciences*, vol. 113, no. 1, pp. 23–31, 2010.
- [6] Q. Q. Liang, D. F. Ding, Z. J. Xi et al., "Protective effect of ligustrazine on lumbar intervertebral disc degeneration of rats induced by prolonged upright posture," *Evidence-based complementary and alternative medicine: eCAM*, vol. 2014, Article ID 508461, 9 pages, 2014.
- [7] X. T. Wang, X. J. Sun, C. Li et al., "Establishing a cell-based high-content screening assay for TCM compounds with anti-renal fibrosis effects," *Evidence-Based Complementary and Alternative Medicine*, vol. 2018, Article ID 7942614, 10 pages, 2018.
- [8] Q. Bian, A. Jain, X. Xu et al., "Excessive activation of TGF $\beta$  by spinal instability causes vertebral endplate sclerosis," *Scientific Reports*, vol. 6, no. 1, Article ID 27093, 2016.
- [9] S. Liu, B. Zhao, H. Shi et al., "Ligustrazine inhibits cartilage endplate hypertrophy via suppression of TGF- $\beta$ 1," *Evidence-Based Complementary and Alternative Medicine*, vol. 2016, Article ID 1042489, 9 pages, 2016.
- [10] Q. Q. Liang, Q. Zhou, M. Zhang et al., "Prolonged upright posture induces degenerative changes in intervertebral discs in rat lumbar spine," *Spine*, vol. 33, no. 19, pp. 2052–2058, 2008.
- [11] K. Masuda, Y. Aota, C. Muehleman et al., "A novel rabbit model of mild, reproducible disc degeneration by an annulus needle puncture: correlation between the degree of disc injury and radiological and histological appearances of disc degeneration," *Spine*, vol. 30, no. 1, pp. 5–14, 2005.
- [12] C. M. Tran, D. Markova, H. E. Smith et al., "Regulation of CCN2/connective tissue growth factor expression in the nucleus pulposus of the intervertebral disc: role of Smad and activator protein 1 signaling," *Arthritis & Rheumatism*, vol. 62, no. 7, pp. 1983–1992, 2010.
- [13] J. Bedore, W. Sha, M. R. McCann, S. Liu, A. Leask, and C. A. Séguin, "Impaired intervertebral disc development and premature disc degeneration in mice with notochord-specific deletion of CCN2," *Arthritis & Rheumatism*, vol. 65, no. 10, pp. 2634–2644, 2013.
- [14] W. M. Erwin, "The Notochord, notochordal cell and CTGF/CCN-2: ongoing activity from development through maturation," *Journal of Cell Communication and Signaling*, vol. 2, no. 3-4, pp. 59–65, 2008.
- [15] C. M. Tran, Z. R. Schoepflin, D. Z. Markova et al., "CCN2 suppresses catabolic effects of interleukin-1 $\beta$  through  $\alpha$ 5 $\beta$ 1 and  $\alpha$ V $\beta$ 3 integrins in nucleus pulposus cells," *Journal of Biological Chemistry*, vol. 289, no. 11, pp. 7374–7387, 2014.
- [16] T. Nishida, H. Kawaki, R. M. Baxter, R. A. DeYoung, M. Takigawa, and K. M. Lyons, "CCN2 (Connective Tissue Growth Factor) is essential for extracellular matrix production and integrin signaling in chondrocytes," *Journal of Cell Communication and Signaling*, vol. 1, no. 1, pp. 45–58, 2007.
- [17] M. V. Risbud and I. M. Shapiro, "Notochordal cells in the adult intervertebral disc: new perspective on an old question," *Critical Reviews™ in Eukaryotic Gene Expression*, vol. 21, no. 1, pp. 29–41, 2011.
- [18] M. L. Ji, H. Jiang, X. J. Zhang et al., "Preclinical development of a microRNA-based therapy for intervertebral disc degeneration," *Nature Communications*, vol. 9, no. 1, p. 5051, 2018.
- [19] Z. Li, X. Li, C. Chen et al., "Melatonin inhibits nucleus pulposus (NP) cell proliferation and extracellular matrix (ECM) remodeling via the melatonin membrane receptors mediated PI3K-Akt pathway," *Journal of Pineal Research*, vol. 63, no. 3, Article ID e12435, 2017.
- [20] S. Xiao, K. H. Li, and H. B. Lu, "Effect of ligustrazine on the expression of Bcl-2 protein and apoptosis in rabbit articular chondrocytes in monolayer culture," *Hunan yi ke da xue xue*

bao = Hunan yike daxue xuebao = *Bulletin of Hunan Medical University*, vol. 28, no. 3, pp. 224–226, June 2003.

- [21] X.-D. Ju, M. Deng, Y.-F. Ao et al., “The protective effect of tetramethylpyrazine on cartilage explants and chondrocytes,” *Journal of Ethnopharmacology*, vol. 132, no. 2, pp. 414–420, 2010.
- [22] Y. Jiang, C. Liu, W. Chen, H. Wang, C. Wang, and N. Lin, “Tetramethylpyrazine enhances vascularization and prevents osteonecrosis in steroid-treated rats,” *BioMed Research International*, vol. 2015, Article ID 315850, 12 pages, 2015.
- [23] W. J. Wang, L. Yang, X. H. Wang, and H. L. Li, “Effect of ligustrazine on airway remodeling in asthmatic rats,” *Zhonghua jie he he hu xi za zhi = Zhonghua jiehe he huxi zazhi = Chinese journal of tuberculosis and respiratory diseases*, vol. 27, no. 12, pp. 833–836, 2004.
- [24] M. Lu, J. Zhou, F. Wang et al., “Effect of tetramethylpyrazine on expression of Smad7 and SnoN in rats with UUO,” *Zhongguo Zhong yao za zhi = Zhongguo zhongyao zazhi = China Journal of Chinese Materia Medica*, vol. 34, no. 1, pp. 84–88, 2009.
- [25] X.-P. Yuan, L.-S. Liu, Q. Fu, and C.-X. Wang, “Effects of ligustrazine on ureteral obstruction-induced renal tubulointerstitial fibrosis,” *Phytotherapy Research*, vol. 26, no. 5, pp. 697–703, 2012.
- [26] B. Lu, L. Yu, S. Li et al., “Alleviation of CCl<sub>4</sub>-induced cirrhosis in rats by tetramethylpyrazine is associated with down-regulation of leptin and TGF- $\beta$ 1 pathway,” *Drug and Chemical Toxicology*, vol. 33, no. 3, pp. 310–315, 2010.
- [27] H. Yang, J. Li, N. Xing et al., “Effect of tetramethylpyrazine and rat CTGF miRNA plasmids on connective tissue growth factor, transforming growth factor-beta in high glucose stimulated hepatic stellate cells,” *Sheng wu yi xue gong cheng xue za zhi = Journal of biomedical engineering = Shengwu yixue gongchengxue zazhi*, vol. 31, no. 2, pp. 394–399, 2014.
- [28] J. Li, N. Dong, S. Cheng et al., “Tetramethylpyrazine inhibits CTGF and Smad2/3 expression and proliferation of hepatic stellate cells,” *Biotechnology, Biotechnological Equipment*, vol. 29, no. 1, pp. 124–131, 2015.
- [29] H. Zhang, Y. Song, Z. Li et al., “Evaluation of ligustrazine on the prevention of experimentally induced abdominal adhesions in rats,” *International Journal of Surgery*, vol. 21, pp. 115–121, 2015.



Hindawi

Submit your manuscripts at [www.hindawi.com](http://www.hindawi.com)

